Association of glial fibrillary acid protein, Alzheimer's disease pathology and cognitive decline

Débora E. Peretti,[1] Cecilia Boccalini,[1] Federica Ribaldi,[2,3] Max Scheffler,[4] Moira Marizzoni,[5] Nicholas J. Ashton,[6,7,8,9] Henrik Zetterberg,[9,10,11,12,13,14] Kaj Blennow,[7,12,15,16] Giovanni B. Frisoni,[2,3] and Valentina Garibotto[1,17,18]

Abstract

Increasing evidence shows that neuroinflammation is a possible modulator of tau spread effects on cognitive impairment in Alzheimer's disease. In this context, plasma levels of the glial fibrillary acidic protein (GFAP) have been suggested to have a robust association with Alzheimer's disease pathophysiology. This study aims to assess the correlation between plasma GFAP and Alzheimer's disease pathology, and their synergistic effect on cognitive performance and decline.

A cohort of 122 memory clinic subjects with amyloid and tau positron emission tomography, MRI scans, plasma GFAP, and Mini-Mental State Examination (MMSE) was included in the study. A subsample of 94 subjects had a follow-up MMSE score at least one year after baseline. Regional and voxel-based correlations between Alzheimer's disease biomarkers and plasma GFAP were assessed. Mediation analyses were performed to evaluate the effects of plasma GFAP on the association between amyloid and tau PET, and tau PET and cognitive impairment and decline.

GFAP was associated with increased tau PET ligand uptake in the lateral temporal and inferior temporal lobes in a strong left-sided pattern independently of age, gender, education, amyloid, and APOE status (β=0.001, p<0.01). The annual rate of MMSE change was significantly and independently correlated with both GFAP (β=0.006, p<0.01) and global tau SUVR (β=4.33, p<0.01), but not with amyloid burden. Partial mediation effects of GFAP were found on the association between amyloid and tau pathology (13.7%), and between tau pathology and cognitive decline (17.4%), but not on global cognition at baseline.

Neuroinflammation measured by circulating GFAP is independently associated with tau Alzheimer's disease pathology and with cognitive decline, suggesting neuroinflammation as a potential target for future disease-modifying trials targeting tau pathology.

Author affiliations

1 Laboratory of Neuroimaging and Innovative Molecular Tracers (NIMTlab), Geneva University Neurocentre and Faculty of Medicine, University of Geneva, Geneva 1205, Switzerland

2 Laboratory of Neuroimaging of Aging (LANVIE), University of Geneva, Geneva 1205, Switzerland

3 Geneva Memory Centre, Department of Rehabilitation and Geriatrics, Geneva University Hospitals, Geneva 1205, Switzerland

4 Division of Radiology, Geneva University Hospitals, Geneva 1205, Switzerland

5 Biological Psychiatry Unit, IRCCS Istituto Centro San Giovanni di Dio Fatebenefratelli, Brescia 25125, Italy

6 Centre for Age-Related Medicine, Stavanger University Hospital, Stavanger 4011, Norway

7 Department of Psychiatry and Neurochemistry, Institute of Neuroscience and Physiology, The Sahlgrenska Academy at the University of Gothenburg, Mölndal 413 90, Sweden

8 King's College London, Institute of Psychiatry, Psychology & Neuroscience, Maurice Wohl Clinical Neuroscience Institute, London SE5 9RX, UK

9 NIHR Biomedical Research Centre for Mental Health & Biomedical Research Unit for Dementia at South London & Maudsley NHS Foundation, London SE5 8AF, UK

10 UK Dementia Research Institute at UCL, London WC1E 6BT, UK

11 Department of Neurodegenerative Disease, UCL Institute of Neurology, London WC1N 3BG, UK

12 Clinical Neurochemistry Laboratory, Sahlgrenska University Hospital, Mölndal 413 45, Sweden

13 Hong Kong Centre for Neurodegenerative Diseases, Clear Water Bay, Hong Kong Units 1501-1502, 1512-1518, China

14 Wisconsin Alzheimer's Disease Research Centre, University of Wisconsin School of Medicine and Public Health, University of Wisconsin-Madison, Madison, WI 53792, USA

15 Paris Brain Institute, ICM, Pitié Salpêtrière Hospital, Sorbonne University, Paris 75013, France

16 Neurodegenerative Disorder Research Centre, Division of Life Sciences and Medicine, and Department of Neurology, Institute on Aging and Brain Disorders, University of Science and Technology of China and First Affiliated Hospital of USTC, Hefei 230001, China

17 Division of Nuclear Medicine and Molecular Imaging, Geneva University Hospitals, Geneva 1205, Switzerland

18 Centre for Biomedical Imaging, University of Geneva, Geneva 1205, Switzerland

Correspondence to: Débora Elisa Peretti

Rue Gabrielle-Perret-Gentil 4, 1205 Genève, Switzerland

E-mail: Debora.Peretti@unige.ch

Running title: Association of GFAP and AD pathology

Keywords: neurofibrillary tau tangles; Alzheimer's disease biomarkers; glial fibrillary acidic protein; cognitive decline; positron emission tomography

Introduction

Alzheimer's disease is a neurodegenerative disorder biologically defined by the presence of amyloid-β plaques and hyperphosphorylated tau protein deposition.[1] Positron emission tomography (PET) is an imaging technique that allows for the *in vivo* visualisation and quantification of AD pathology.[2] Furthermore, it also allows not only for the discrimination of Alzheimer's disease from other neurodegenerative disorders,[3,4] but also for the staging of Alzheimer's disease based on characteristic pathology distribution in the brain.[5,6] More specifically, the spatial distribution of tau aggregates has been linked to cognitive impairment and neurodegeneration.[5,7,8]

However, in addition to these established Alzheimer's disease biomarkers, studies have shown that neuroinflammation coexists with characteristic Alzheimer's disease pathology.[9,10] In specific, astrocyte reactivity is commonly found enclosing amyloid pathology in Alzheimer's disease patients.[11,12] This association is so established that the National Institute on Ageing and the Alzheimer's Association (NIA-AA) is proposing revised criteria for diagnosis and staging of Alzheimer's Disease, where amyloid and tau pathology still remain as the main biomarkers for disease identification, but neuroinflammation is now introduced, together with neurodegeneration, as a staging and prognosis biomarker.[13,14]

While astrocyte reactivity has been mainly related to amyloid pathology,[12] studies have also suggested that neuroinflammation drives tau pathology propagation in the brain,[15,16] thereby following the stereotyped spread in Braak stages.[17] Even though an association between neuroinflammation and tau pathology is known, additional investigation in settings closer to clinical routine are still required for the perspective of a successful clinical implementation of neuroinflammation biomarkers.

The neuroinflammatory response caused by Alzheimer's disease pathology may be assessed through the circulatory markers glial fibrillary acidic protein (GFAP).[12,18] GFAP expression measured in plasma is used for the *in vivo* identification of astroglia and, an increase of this marker is a typical indication of the presence of pathology in the central nervous system.[19,20] Furthermore, plasma GFAP levels have been suggested to be a sensitive biomarker for detecting reactive astrogliosis.[21–23] Beyond its link with neurodegenerative disorders, previous studies have also shown that GFAP is associated with deficits and decline in several cognitive domains.[24,25] Consequently, the NIA-AA has included GFAP as a staging biomarker for neuroinflammation in the abovementioned revised criteria.[13]

Previous studies have shown that plasma GFAP levels are associated with Alzheimer's disease pathology measured in cerebrospinal fluid (CSF),[12,21,26,27] plasma,[21,26,28] and neuroimaging.[12,29] More specifically, GFAP has been suggested to play a role in the association between amyloid pathology and early deposition of neurofibrillary tau tangles.[26] Moreover, GFAP has been shown to predict conversion from mild cognitive impairment to Alzheimer's disease dementia.[27]

The aim of this study was to further investigate the association between Alzheimer's disease pathology (i.e., amyloid and tau accumulation) measured through PET imaging, and plasma GFAP in a memory clinic cohort. Furthermore, the correlation between GFAP and cognitive

performance and decline was also assessed. Finally, as neuroinflammation and Alzheimer's disease pathology have been suggested to be closely related, a mediation analysis of the GFAP effect in the association between amyloid and tau, and the association between tau and cognitive performance and decline was studied.

Materials and methods

Subjects

A cohort of 122 subjects who consulted the Memory Clinic of the Geneva University Hospitals (HUG, Geneva, Switzerland) was included in this study. Each subject underwent the memory clinic's workup, including clinical and neurological assessment, neuropsychological testing, and 3D T1 MRI. Additional procedures, such as amyloid PET, tau PET, and blood sampling have been performed if deemed clinically useful, or in the context of other research projects. Subjects were clinically classified as cognitively unimpaired (CU), mild cognitive impaired (MCI),[30] or dementia.[31] Inclusion criteria were: (1) amyloid and tau PET imaging performed within 12 months of each other (average 4 ± 6 months), (2) 3D T1 MRI scans performed within 12 months from tau PET images (average 4 ± 8 months), (3) neuropsychological assessment with at least one Mini-Mental State Examination (MMSE) performed within 12 months of tau PET imaging (average 3 ± 5 months), and (4) plasma GFAP levels assessed within 12 months from tau PET (average 2 ± 8 months).

A subsample of 94 subjects was included who had a follow-up neuropsychological assessment including at least MMSE scores after at least 12 months after baseline (average 27 ± 15 months). Annual rate of MMSE score change was calculated and cognitive decline was defined as an average annual rate of MMSE change of 1 point per year.[32]

The local review board (Cantonal Commission of Research Ethics, Geneva, Switzerland) approved the studies, which were conducted in concordance with the principles of the Declaration of Helsinki and International Conference on Harmonisation Good Clinical Practice. All subjects or their relatives provided voluntary written informed consent to share their data for research purposes.

Imaging Acquisition and Processing

MRI examinations were performed at the HUG's Division of Radiology. 3D T1 images were acquired using a Magnetom Skyra 3 Tesla scanner (Siemens Healthineers, Erlangen, Germany) equipped with a 64-channel head coil and were acquired in concordance with IMI pharmacog WP5/European ADNI sequences and published procedures.[33] A field of view of 256 mm, 0.9-1 mm slice thickness, 1819-1930 ms repetition time, 2.19-2.4 ms echo time, 8° flip angle, and no fat suppression were used.

PET imaging was performed at the Nuclear Medicine and Molecular Imaging Division of the HUG. All images were acquired using a Biograph PET/CT scanner (Siemens Health Solutions, Malvern, PA, USA), reconstructed using a 3D OSEM algorithm (4 iterations, 8 subsets), a 2 mm Gaussian convolution kernel, corrected for dead time, normalisation, attenuation, and sensitivity. All radiotracers are commercially available, were synthesised at radiopharmaceutical Good Manufacturing Practice laboratories and shipped to Geneva. For amyloid PET, 41 subjects were injected with 207 ± 23 MBq [^{18}F]florbetapir, and images were acquired 40 min after intravenous administration of the radiotracer for 10 min. The remaining 81 subjects were scanned using 172 ± 18 MBq of [^{18}F]flutemetamol, and images were acquired 90 min after intravenous radiotracer injection for 20 min. For tau PET, [^{18}F]flortaucipir, synthesised at the Centre for Radiopharmaceutical Sciences in Villigen, Switzerland, under license from the intellectual property owner (Avid subsidiary of Lilly, Philadelphia, PA, USA), was used. Subjects were injected with 207 ± 50 MBq intravenously and images were acquired 75 min after injection for 30 min.

All images were processed at the Memory Clinic of the HUG using SPM12 (Wellcome Trust Centre for Neuroimaging, London, UK) and MATLAB R2018b version 9.5 (MathWorks Inc., Sherborn, USA). Firstly, 3D T1 MRI images were aligned to the anterior commissure – posterior commissure line. Then, they were normalised to the Montreal Neurologic Institute (MNI) space using tissue probability maps.[34] PET images were aligned to the subject's respective MRI image and then, using the transformation matrix estimated for the MRI scans, they were transformed into the MNI space. Volumes of interest (VOI) were defined based on the automated anatomic labelling atlas 3.[35]

Amyloid PET images were converted to standardised uptake value ratios (SUVR) using the whole cerebellum as a reference region. Average SUVR was extracted from the Centiloid

VOI and converted to Centiloid units[36–38] so that data from different radiotracers could be equally compared. A Centiloid value of 12 was used to define amyloid positivity (A+).[39,40]

Tau PET images were converted to SUVR values using the cerebellar crus as a reference region.[41,42] Tau positivity was defined based on the Simplified Temporal-Occipital Classification (STOC) model.[40,42] Average SUVR was extracted based on a global set of regions (amygdala, parahippocampus, middle occipital gyrus, and temporal inferior gyrus[43]) and in Braak regions (weighted averages of the following bilateral regions: Braak I/II: hippocampus; Braak III: parahippocampal gyrus, lingual gyrus, amygdala; Braak IV: inferior temporal cortex, middle temporal cortex, temporal pole, thalamus, posterior cingulate, insula; Braak V: frontal cortex, parietal cortex, occipital cortex, superior temporal cortex, precuneus, caudate nucleus, putamen; Braak VI: precentral gyrus, postcentral gyrus, paracentral gyrus, cuneus[44]).

Cortical reconstruction and volumetric segmentation of T1 MRI images were performed using Freesurfer (v7, recon-all[45]). An Alzheimer's disease cortical signature (weighted average cortical thickness in the entorhinal, inferior temporal, middle temporal, and fusiform VOIs) was created.[46]

Plasma Sampling and Processing

Plasma samples were collected within a year of tau PET examination, with participants non-fasting. Blood was collected in EDTA-plasma tubes and centrifuged (2000*g*, +4ºC for 10 min). Following centrifugation, plasma was aliquoted into 1.5 ml polypropylene tubes (1 ml plasma in each tube) and stores at -80ºC in polypropylene tubes. GFAP levels were assessed using GFAP Simoa Discovery kits for HD-X (Quanterix, Billerica, MA).[12,47]

Statistical Analyses

Subjects were classified into AT profiles based on their combined amyloid and tau statuses. A Kruskal-Wallis test and Dunn tests for multiple corrections using Benjamin-Hochberg were performed to explore differences in age, years of education, MMSE, Centiloid, global tau SUVR, composite Alzheimer's disease cortical thickness signature, and plasma GFAP levels between groups. A chi-square test was used to compare gender and APOE carriership differences across the groups. Significant differences between baseline and follow-up MMSE scores were assessed using a paired Wilcoxon test for each group individually.

Spearman correlations between GFAP levels and Centiloid, global and regional Braak tau SUVR, cortical thickness, and MMSE scores at baseline were calculated for the complete data and per AT profile. Regional tau SUVR correlations with GFAP were also computed for right and left hemispheres separately. A multivariate linear regression model to assess the association between GFAP levels and global tau and Centiloid was performed, correcting for age, gender, education, APOE carriership, and cortical thickness.

A voxel-wise regression to assess the correlation between GFAP and tau SUVR at a voxel level was performed, controlling for age, gender, education, APOE carriership, and Centiloid. Finally, a voxel-wise linear regression to assess the correlation between GFAP and amyloid SUVR (per amyloid radiotracer) was performed, controlling for age, gender, education, APOE carriership, and global tau SUVR. Statistical threshold for voxel-based analyses was set at $P = 0.001$, FWE-corrected at the cluster level. A second model was run including also baseline MMSE scores as a nuisance variable.

Spearman correlations were used to assess the correlation between baseline MMSE and MMSE annual rate of change and Centiloid, global tau SUVR, and GFAP for the complete data and by AT profiles. A multivariate linear regression model was used to assess the association between the same variables, corrected for age, gender, education, APOE carriership, and cortical thickness. Differences in plasma GFAP levels between decliners and stable individuals were assessed using a Wilcoxon test for the whole cohort and by AT status.

To examine whether the associations between Centiloid and global tau SUVR were mediated by GFAP levels, we performed mediation analyses controlling for age, gender, education, and APOE carriership. Additional mediation analyses were run to examine if the association between regional Braak tau SUVR and Centiloid, the association between global tau SUVR and MMSE scores, and the association between Centiloid and MMSE scores were mediated by GFAP levels. Mediation analysis was also performed to test whether the relationship between global tau SUVR or Centiloid and MMSE annual rate of change was mediated by GFAP levels, again correcting for age, gender, education, and APOE carriership. Bootstrapping resampling was used to estimate confidence intervals for all mediation analyses with 1000 resampling.[48]

A *P*-value of 0.05 was considered as the significance threshold for all analyses, which were performed using RStudio (version "Mountain Hydrangea", R version 4.3.1). Dunn tests were performed using the package *FSA* (version 0.9.4), multilinear regression was performed using

the package *lme4* (version 1.1), and mediation analysis using the package *mediation* (version 4.5.0). Voxel-wise analysis was run in MATLAB (R2023b version 9.12) using SPM12.

Results

Population

Characteristics of the included cohort of subjects at baseline is shown in **Table 1** per AT profile. The average age of the population was 72 ± 8 years, 61 individuals were females (50%), average education was 14 ± 4 years, MMSE score at baseline was 26 ± 4, Centiloid was 49 ± 44 units, global tau SUVR was 1.34 ± 0.34, cortical thickness was 2.70 ± 0.18 mm, and GFAP levels were 188.2 ± 114.4 pg/ml. Age and gender were significantly different between groups, but no significant differences were found when correcting for multiple comparisons.

For the subsample of subjects with a follow-up neuropsychological assessment, the average MMSE score was of 24 ± 5, with an average rate of change of 1 ± 2 MMSE points per year. A significant difference between MMSE scores was found at baseline and follow-up ($P < 0.01$). When stratifying subjects by AT profile, only the A+T- and A+T+ groups showed significantly different MMSE scores at follow-up when compared to baseline ($P < 0.01$). No significant differences in age or gender were found between the declining group of subjects and the stable individuals.

Correlation Analyses and Multilinear Regressions at Baseline

Figure 1 shows the difference in GFAP values across AT profiles. Correlation between Centiloid and GFAP values was significant (**Table 2**). However, when stratifying subjects by AT profile, the correlation was not significant for any of the profiles (**Supplementary Table 1**). Correlation between global tau SUVR and GFAP levels was also significant (**Table 2**). When stratifying subjects by AT profile, only the A+T+ subjects showed a significant correlation between variables (r = 0.45, $P < 0.01$, **Supplementary Table 1**). Regional tau SUVR values were also significantly correlated to GFAP levels, with the exception of Braak VI (**Table 2**). When stratified by AT profile, only the A+T+ group showed significant results (Braak III: 0.37, $P = 0.01$; Braak IV: 0.34, $P = 0.02$, Braak V: 0.30, $P = 0.04$), with the Braak I/II and VI not showing significant correlations for any of the profiles (**Supplementary Table**

1). Cortical thickness (r= -0.34, $P < 0.01$) and baseline MMSE scores (r = -0.34, $P < 0.01$) showed an inverse correlation with GFAP levels (**Table 2**), but when dividing subjects by AT profile, no significant correlations were found (**Supplementary Table 1**). Multivariate linear regression showed a significant positive association between plasma GFAP levels and age (β = 4.1, $P < 0.01$), global tau SUVR (β = 89.4, $P = 0.01$), and cortical thickness (β = -119.9, $P = 0.04$). The remaining variables (Centiloid, gender, education, and APOE carriership) were not significantly associated with GFAP.

Significant differences in tau PET SUVR uptake between right and left hemispheres were found for the global and Braak III, IV, and VI VOIs, with the left hemisphere showing a bigger uptake. When correlating plasma GFAP levels with tau PET SUVR uptake by right and left hemispheres separately, similar results were found as for the bilateral VOIs. Significant correlations were found for the global (right: r = 0.38, $P < 0.01$; left: r = 0.40, $P < 0.01$), Braak III (right: r = 0.38, $P < 0.01$; left: r = 0.38, $P < 0.01$), Braak IV (right: r = 0.35, $P < 0.01$; left: r = 0.39, $P < 0.01$), Braak V (right: r = 0.33, $P < 0.01$; left: r = 0.34, $P < 0.01$), and Braak VI left (r = 0.21, $P < 0.01$) VOIs. Braak I/II (right: r = 0.11, $P = 0.22$; left: r = 0.15, $P = 0.11$) and Braak VI right (r = 0.17, $P = 0.06$) VOIs were not significantly correlated to plasma GFAP.

Topographical Association Between Tau SUVR and GFAP

The hypothesis that plasma GFAP is associated with greater tau PET uptake independently of amyloid burden (measured through Centiloid values) was tested using a voxel-wise multilinear regression model. Results revealed that plasma GFAP was associated with increased tau PET SUVR values in the lateral temporal and frontal regions of the brain (false discovery rate corrected at $P < 0.01$; significant clusters: β = 0.001), with the left side of the brain showing higher correlations than the right (**Figure 2**). These results were independent of age, gender, education, amyloid burden, and APOE genotype. The association between tau PET uptake and plasma GFAP levels did not significantly change when including baseline MMSE score as a covariate (**Supplementary Figure 1**). No clusters were found to be significantly correlated to GFAP for any of the amyloid radiotracers.

Correlation Analysis and Multilinear Regressions at Follow-Up

At baseline, all imaging biomarkers and plasma GFAP levels were significantly correlated with MMSE scores (**Supplementary Table 2**). MMSE annual rate of change was

significantly correlated to Centiloid, global tau SUVR, cortical thickness, and plasma GFAP levels (**Table 3**). When dividing tau uptake by Braak regions, only the uptake in Braak VI region was not significantly correlated to the annual rate of MMSE change (**Table 3**). When separating subjects into AT profiles, the A+T+ group presented significant correlations between annual rate of MMSE change with global tau SUVR (r = 0.5, $P < 0.01$), Braak III (r = 0.37, $P = 0.04$), Braak IV (r = 0.48, $P < 0.01$), cortical thickness (r = -0.55, $P < 0.01$), and plasma GFAP (r = 0.37, $P = 0.05$), but not with Centiloid, Braak I/II, Braak V, and Braak VI. A-T-, A-T+, and A+T- subjects did not present significant correlations for Centiloid, global tau SUVR, Braak regional SUVR, cortical thickness, and plasma GFAP. Multivariate linear regression showed a significant positive association between MMSE annual rate of change and global tau SUVR ($\beta = 3.24$, $P < 0.01$), plasma GFAP ($\beta = 0.005$, $P < 0.01$), and with cortical thickness ($\beta = -2.43$, $P = 0.04$). Wilcoxon test showed that plasma GFAP levels were significantly higher in individuals that declined cognitively than in the ones who did not in the whole sample ($P < 0.01$, **Supplementary Figure 2A**), and only for the A-T- and A+T+ profiles (**Supplementary Figure 2B**).

Mediation Analysis

Figure 3A shows path diagrams assessing plasma GFAP as a potential mediator of the associations between Centiloid and global tau SUVR. A statistically significant mediation effect was found (9.1% [95% CI: 0.8% – 24%] of the total effect, $P = 0.02$). Mediation effects of plasma GFAP in the association between global tau SUVR and baseline MMSE scores were not significant ($P = 0.24$), while the direct effects were (-5.08, $P < 0.01$). Mediation effects of plasma GFAP in the association between Centiloid and baseline MMSE were not significant ($P = 0.08$), while the direct effects were (-0.02, $P < 0.01$). When assessing the mediation of plasma GFAP (**Figure 3B**) in the association between global tau SUVR and the annual rate of MMSE change, a statistically significant mediation effect was also found (14.1% [95% CI: 2.2% – 31%] of the total effect, $P = 0.01$). When assessing the mediation of plasma GFAP in the association between Centiloid and the MMSE annual rate of change, no significant effects were found.

Mediation analysis by Braak region SUVR instead of global tau PET SUVR showed that plasma GFAP mediated the effects of Centiloid in regional tau SUVR in Braak III (12.2% [95% CI: 1.1% – 33%] of the total effect, $P = 0.04$), Braak IV (10.0% [95% CI: 1.6% – 26%] of the total effect, $P = 0.02$), and Braak V (13.8% [95% CI: 1.9% – 36%] of the total effect, P

= 0.01), but not in Braak I/II (P = 0.94, direct effect = 0.0006 P < 0.01) and Braak VI (P = 0.12, direct effect = 0.0003 P < 0.01).

Discussion

The main goal of this study was to evaluate the association between Alzheimer's disease pathology measured by PET and plasma GFAP concentration as a measure of neuroinflammation in a memory clinic cohort. To this end, an investigation of the association between amyloid and tau PET SUVR and plasma GFAP was performed both at regional and voxel level. In general, plasma GFAP was associated with tau deposition mainly in the temporal and inferior frontal lobes, with stronger correlations on the left side of the brain. Furthermore, neuroinflammation measured through GFAP was found to have a partial mediation effect in the studied associations between Centiloid values and tau PET SUVR and with the annual rate of MMSE change globally.

Alzheimer's disease pathology is known to trigger a neuroinflammatory process in the brain that results not only in activated microglia that cannot phagocyte amyloid deposits, leading to plaque accumulation,[49,50] but also to astrocytic changes in the blood-brain barrier that further impair plaque clearance from the brain.[51] Therefore, neuroinflammation associated with Alzheimer's disease pathology might be of a higher influence than previously considered. The inclusion of plasma GFAP as an inflammation marker in most recent revisions of the ATN profile classification is an initial step for further understanding the complex interplay of the brain's response to pathological deposits.

GFAP levels can be measured not only through plasma but also through CSF samples. Previous studies have found that both are markers of neuroinflammation, and measures are correlated, even if GFAP levels behave differently at each stage of the Alzheimer's disease spectrum when measured through different assays.[12,21] It has further been suggested that while plasma GFAP reflects neuroinflammation caused by reactive astrogliosis due to amyloid deposits, CSF GFAP is associated with astrocyte response to neuroinflammatory changes.[21] Finally, a previous study has found that CSF is an unreliable method to measure GFAP in Alzheimer's disease, whereas plasma GFAP is a stable matrix.[52] Therefore, caution must be taken when comparing results of studies with different GFAP measuring methods.

When binarizing subjects according to biomarker positivity in AT profiles, it is possible to observe that individuals without the presence of Alzheimer's disease pathology present significantly lower plasma GFAP levels compared to patients with Alzheimer's disease pathology. However, no difference was found between A+T- and A+T+ groups, in line with previous results and suggesting that GFAP increase represents an early event in Alzheimer's disease pathogenesis.[12] While results in the previous section agree with the strong correlation between plasma GFAP and amyloid pathology, it was also found that amyloid PET distribution was not significantly correlated to GFAP at a voxel level when corrected for other covariates. Furthermore, the correlation between GFAP levels and PET biomarkers was significant in general, but it is interesting to notice that when stratifying by AT profile, tau PET uptake remained significantly correlated with GFAP levels, suggesting that plasma GFAP is not only associated with amyloid deposition, in contrast with what has been suggested by previous studies.[12,53,54] Finally, in agreement with a previous study, plasma GFAP was more strongly correlated with longitudinal cognitive decline than measurements of brain atrophy.[55] It is important to point out that the association between plasma GFAP and tau PET was independent of age, gender, education, MMSE, Centiloid, and cortical thickness.

The threshold choice for amyloid deposition in this study was based on previous literature that matches the local sample at the Geneva Memory Clinic. Nonetheless, other thresholds have been suggested in the literature, and these choices are mostly related to the endpoint of the study being performed. While lower threshold points, such as the one used in this study, perform well in prevention studies[56] and seem to be a better fit for APOE4 carrier patient selection for anti-amyloid studies,[57] higher thresholds usually have the best agreement with neuropathological and clinicopathological evidence of AD.[58] Therefore, the selection of centiloid threshold for amyloid status binarization should be carefully assessed, taking into consideration study design and primary endpoint.

The association between neuroinflammation and global tau PET uptake as a marker has been previously investigated. However, regional SUVR values have shown different association strengths and significance between biomarkers. The correlation between plasma GFAP and regional tau PET SUVR being present in only specific regions further support the use of it as a potential staging biomarker when combined with amyloid and tau. Moreover, plasma GFAP was significantly associated with cognitive decline, independently of demographic and pathology characteristics, further promoting its use to assess individual prognosis. However, it is important to mention that elevated levels of GFAP have been consistently reported in

other neurodegenerative diseases. Indeed, a combination with other biomarkers seems to be an essential condition for the putative use of GFAP as a biomarker in Alzheimer's disease.[26] While the results found that global tau SUVR is significantly correlated to cognitive decline are in line with previous studies,[59] they also support the hypothesis that assessing regional tau uptake instead might offer a better prognostic value of disease progression. However, that remains to be corroborated by future studies.

The topographical association between plasma GFAP levels and tau SUVR distribution further highlights the importance of considering regional PET uptake in favour of global values. A lateralised association was found (**Figure 2**) between markers, which could be related to the asymmetric and heterogenous brain distribution of tau aggregates.[60] Furthermore, a lateralisation of tau PET SUVR uptake was also found, with significant differences between the right and left hemispheres in some brain regions. Previous studies have found that brain structure changes throughout the Alzheimer's disease continuum in a lateralised direction, with the left side of the brain being more affected than the right especially in the temporal lobe.[61–63] This larger atrophy on the left temporal lobe affects the functional connectivity of this region to the rest of the brain. As it has been already shown that the loss of functional connectivity is correlated to a larger tau accumulation,[64] one might expect a larger correlation between neuroinflammation, as a result of Alzheimer's disease pathology, and tau aggregates in the left hemisphere. A stronger correlation between tau aggregation and neuroinflammation was mainly localised in regions known for typical Alzheimer's disease accumulation. This raises the question of whether different correlation patterns could be found for other tauopathies that can also be studied using tau PET imaging.[65,66]

Previous studies have suggested that plasma GFAP could be used as an earlier marker than tau PET in hypothetical models of Alzheimer's disease progression.[12,26] Results in the previous section concur with these results by showing that GFAP mediates the effect of amyloid deposition on tau pathology, in line also with earlier studies that concluded that astrocytic activation could facilitate tau pathology spread. Mediation analysis further results in only partial mediation effects, indicating the possible presence of other factors that could mediate the studied effects, such as other neuroinflammation markers (i.e., microglial activation) and genetic factors (i.e., apolipoprotein E4 carriership).

Current disease-modifying clinical trials mostly include the use of anti-amyloid drugs.[67–69] However, future clinical trials targeting tau aggregates are expected to emerge in the coming

years,[70] It will be important to take into consideration the neuroinflammatory effects of tau pathology in the brain. A possible combination with anti-inflammatory therapies might be of advantage to improve results.

Conclusions from this study are encouraging, however, some limitations still need to be pointed out. Firstly, annual rate of MMSE change was used as a measure for cognitive decline, although MMSE is a global measure characterised by a ceiling effect, being less sensitive in comparison to other neuropsychological tests. Secondly, as this cohort is a sample from a memory clinic, it is enriched in subjects with higher levels of cognitive decline, which also tend to progress at a faster rate. However, the inclusion of a clinical population in this study can also be considered a strength, as it can more easily translate results into clinical practice. Finally, some subgroups depending on the classification used had a low number of subjects (e.g., subjects visually classified in Braak stage VI or the A-T+ population), which could have prevented significant results in subgroup analysis.

Conclusion

Elevated plasma GFAP levels are associated with increased tau deposition in lateral temporal and frontal regions and also with accelerated cognitive decline, independently from tau and amyloid load. GFAP also partially explains the effect of amyloid pathology on tau accumulation and of tau pathology on subsequent cognitive decline. These results support neuroinflammation and astrogliosis as a relevant contributor to Alzheimer's disease pathogenesis, which can be monitored through blood sampling, and suggest neuroinflammation as a potential target for future disease-modifying therapeutic trials targeting tau pathology.

Data availability

The data that support the findings of this study are available from the corresponding author, upon reasonable request.

Acknowledgements

The Clinical Research Centre, at Geneva University Hospital and Faculty of Medicine provides valuable support for regulatory submissions and data management, and the Biobank at Geneva University Hospital for biofluid processing and storage. We thank the Centre for Radiopharmaceutical Sciences of ETH and USZ for providing the PET tracer for tau imaging. We acknowledge Avid radiopharmaceuticals for providing the precursor for the tau radiotracer and emphasise that Avid was not involved in the analysis or interpretation.

Funding

The Centre de la mémoire is funded by the following private donors under the supervision of the Private Foundation of Geneva University Hospitals: A.P.R.A. - Association Suisse pour la Recherche sur la Maladie d'Alzheimer, Genève; Fondation Segré, Genève; Race Against Dementia Foundation, London, UK; Fondation Child Care, Genève; Fondation Edmond J. Safra, Genève; Fondation Minkoff, Genève; Fondazione Agusta, Lugano; McCall Macbain Foundation, Canada; Nicole et René Keller, Genève; Fondation AETAS, Genève.

Competitive research projects have been funded by: H2020 (projects n. 667375), Innovative Medicines Initiative (IMI contract n. 115736 and 115952), IMI2, Swiss National Science Foundation (projects n.320030_185028, n.320030_182772, and n. 320030_169876), VELUX Foundation, and Schmidheiny foundation.

The IRCCS Istituto Centro San Giovanni di Dio Fatebenefratelli in Brescia is partially supported by the Italian Ministry of Health (Ricerca Corrente).

HZ is a Wallenberg Scholar supported by grants from the Swedish Research Council (#2023-00356; #2022-01018 and #2019-02397), the European Union's Horizon Europe research and innovation programme under grant agreement No 101053962, Swedish State Support for Clinical Research (#ALFGBG-71320), the Alzheimer Drug Discovery Foundation (ADDF), USA (#201809-2016862), the AD Strategic Fund and the Alzheimer's Association (#ADSF-21-831376-C, #ADSF-21-831381-C, and #ADSF-21-831377-C), the Bluefield Project, Cure Alzheimer's Fund, the Olav Thon Foundation, the Erling-Persson Family Foundation, Stiftelsen för Gamla Tjänarinnor, Hjärnfonden, Sweden (#FO2022-0270), the European Union's Horizon 2020 research and innovation programme under the Marie Skłodowska-Curie grant agreement No 860197 (MIRIADE), the European Union Joint Programme –

Neurodegenerative Disease Research (JPND2021-00694), the National Institute for Health and Care Research University College London Hospitals Biomedical Research Centre, and the UK Dementia Research Institute at UCL (UKDRI-1003). KB is supported by the Swedish Research Council (#2017-00915 and #2022-00732), the Swedish Alzheimer Foundation (#AF-930351, #AF-939721 and #AF-968270), Hjärnfonden, Sweden (#FO2017-0243 and #ALZ2022-0006), the Swedish state under the agreement between the Swedish government and the County Councils, the ALF-agreement (#ALFGBG-715986 and #ALFGBG-965240), the European Union Joint Program for Neurodegenerative Disorders (JPND2019-466-236), the Alzheimer's Association 2021 Zenith Award (ZEN-21-848495), the Alzheimer's Association 2022-2025 Grant (SG-23-1038904 QC), and the Kirsten and Freddy Johansen Foundation.

Competing interests

VG received research support and speaker fees through her institution from GE Healthcare, Siemens Healthineers, and Novo Nordisk. GBF has received support, payment, consulting fees, or honoraria through his institution for lectures, presentations, speaker bureaus, manuscript writing, or educations events from: Biogen, Roche, Diadem, Novo Nordisk, GE Healthcare, OM Pharma, and Eisai. HZ has served at scientific advisory boards and/or as a consultant for Abbvie, Acumen, Alector, Alzinova, ALZPath, Annexon, Apellis, Artery Therapeutics, AZTherapies, Cognito Therapeutics, CogRx, Denali, Eisai, Merry Life, Nervgen, Novo Nordisk, Optoceutics, Passage Bio, Pinteon Therapeutics, Prothena, Red Abbey Labs, reMYND, Roche, Samumed, Siemens Healthineers, Triplet Therapeutics, and Wave, has given lectures in symposia sponsored by Alzecure, Biogen, Cellectricon, Fujirebio, Lilly, and Roche, and is a co-founder of Brain Biomarker Solutions in Gothenburg AB (BBS), which is a part of the GU Ventures Incubator Program (outside submitted work). KB has served as a consultant and at advisory boards for Acumen, ALZPath, AriBio, BioArctic, Biogen, Eisai, Lilly, Moleac Pte. Ltd, Novartis, Ono Pharma, Prothena, Roche Diagnostics, and Siemens Healthineers; has served at data monitoring committees for Julius Clinical and Novartis; has given lectures, produced educational materials and participated in educational programs for AC Immune, Biogen, Celdara Medical, Eisai and Roche Diagnostics; and is a co-founder of Brain Biomarker Solutions in Gothenburg AB (BBS), which is a part of the GU

Ventures Incubator Program, outside the work presented in this paper. The other authors have no conflicts of interest to disclose.

Supplementary material

Supplementary material is available at *Brain* online.

References

1. Ballard C, Gauthier S, Corbett A, Brayne C, Aarsland D, Jones E. Alzheimer's disease. *The Lancet*. 2011;377(9770):1019-1031. doi:10.1016/S0140-6736(10)61349-9

2. Khoury R, Ghossoub E. Diagnostic biomarkers of Alzheimer's disease: A state-of-the-art review. *Biomark Neuropsychiatry*. 2019;1(November):100005. doi:10.1016/j.bionps.2019.100005

3. Chételat G, Arbizu J, Barthel H, et al. Amyloid-PET and 18F-FDG-PET in the diagnostic investigation of Alzheimer's disease and other dementias. *Lancet Neurol*. 2020;19(11):951-962. doi:10.1016/S1474-4422(20)30314-8

4. Franzmeier N, Neitzel J, Rubinski A, et al. Functional brain architecture is associated with the rate of tau accumulation in Alzheimer's disease. *Nat Commun*. 2020;11(1). doi:10.1038/s41467-019-14159-1

5. Vogel JW, Young AL, Oxtoby NP, et al. Four distinct trajectories of tau deposition identified in Alzheimer's disease. *Nat Med*. 2021;27(5):871-881. doi:10.1038/s41591-021-01309-6

6. Collij LE, Salvadó G, Wottschel V, et al. *Spatial-Temporal Patterns of Amyloid-β Accumulation: A Subtype and Stage Inference Model Analysis*. Vol 0.; 2022. doi:10.1212/wnl.0000000000200148

7. Krishnadas N, Doré V, Robertson JS, et al. Rates of regional tau accumulation in ageing and across the Alzheimer's disease continuum: an AIBL 18F-MK6240 PET study. *EBioMedicine*. 2023;88:104450. doi:10.1016/j.ebiom.2023.104450

8. Ossenkoppele R, Schonhaut DR, Schöll M, et al. Tau PET patterns mirror clinical and neuroanatomical variability in Alzheimer's disease. *Brain*. 2016;139(5):1551-1567. doi:10.1093/brain/aww027

9. Serrano-Pozo A, Mielke ML, Gómez-Isla T, et al. Reactive Glia not only Associates with Plaques but also Parallels Tangles in Alzheimer's Disease. *Am J Pathol*. 2011;179(3):1373-1384. doi:10.1016/j.ajpath.2011.05.047

10. Sheffield LG, Marquis JG, Berman NEJ. Regional distribution of cortical microglia parallels that of neurofibrillary tangles in Alzheimer's disease. *Neurosci Lett*. 2000;285(3):165-168. doi:10.1016/S0304-3940(00)01037-5

11. Osborn LM, Kamphuis W, Wadman WJ, Hol EM. Astrogliosis: An integral player in the pathogenesis of Alzheimer's disease. *Prog Neurobiol*. 2016;144:121-141. doi:10.1016/j.pneurobio.2016.01.001

12. Pereira JB, Janelidze S, Smith R, et al. Plasma GFAP is an early marker of amyloid-β but not tau pathology in Alzheimer's disease. *Brain*. 2021;144(11):3505-3516. doi:10.1093/brain/awab223

13. NIA-AA Workgroup. NIA-AA Revised Criteria for Diagnosis and Staging of Alzheimer's Disease. Published 2023. Accessed October 25, 2023. https://aaic.alz.org/nia-aa.asp

14. Jack CR, Bennett DA, Blennow K, et al. NIA-AA Research Framework: Toward a biological definition of Alzheimer's disease. *Alzheimer's & Dementia*. 2018;14(4):535-562. doi:10.1016/j.jalz.2018.02.018

15. Ising C, Venegas C, Zhang S, et al. NLRP3 inflammasome activation drives tau pathology. *Nature*. 2019;575(7784):669-673. doi:10.1038/s41586-019-1769-z

16. Hopp SC, Lin Y, Oakley D, et al. The role of microglia in processing and spreading of bioactive tau seeds in Alzheimer's disease. *J Neuroinflammation*. 2018;15(1):269. doi:10.1186/s12974-018-1309-z

17. Pascoal TA, Benedet AL, Ashton NJ, et al. Microglial activation and tau propagate jointly across Braak stages. *Nat Med*. 2021;27(9):1592-1599. doi:10.1038/s41591-021-01456-w

18. Prins S, de Kam ML, Teunissen CE, Groeneveld GJ. Inflammatory plasma biomarkers in subjects with preclinical Alzheimer's disease. *Alzheimers Res Ther*. 2022;14(1):106. doi:10.1186/s13195-022-01051-2

19. Colombo E, Farina C. Astrocytes: Key Regulators of Neuroinflammation. *Trends Immunol*. 2016;37(9):608-620. doi:10.1016/j.it.2016.06.006

20. Barro C, Healy BC, Liu Y, et al. Serum GFAP and NfL Levels Differentiate Subsequent Progression and Disease Activity in Patients With Progressive Multiple Sclerosis. *Neurology - Neuroimmunology Neuroinflammation*. 2023;10(1):e200052. doi:10.1212/NXI.0000000000200052

21. Benedet AL, Milà-Alomà M, Vrillon A, et al. Differences Between Plasma and Cerebrospinal Fluid Glial Fibrillary Acidic Protein Levels Across the Alzheimer Disease Continuum. *JAMA Neurol*. 2021;78(12):1471. doi:10.1001/jamaneurol.2021.3671

22. Chatterjee P, Doré V, Pedrini S, et al. Plasma Glial Fibrillary Acidic Protein Is Associated with 18F-SMBT-1 PET: Two Putative Astrocyte Reactivity Biomarkers for Alzheimer's Disease. *Journal of Alzheimer's Disease*. 2023;92(2):615-628. doi:10.3233/JAD-220908

23. Carter SF, Herholz K, Rosa-Neto P, Pellerin L, Nordberg A, Zimmer ER. Astrocyte Biomarkers in Alzheimer's Disease. *Trends Mol Med*. 2019;25(2):77-95. doi:10.1016/j.molmed.2018.11.006

24. Benussi A, Ashton NJ, Karikari TK, et al. Serum Glial Fibrillary Acidic Protein (GFAP) Is a Marker of Disease Severity in Frontotemporal Lobar Degeneration. *Journal of Alzheimer's Disease*. 2020;77(3):1129-1141. doi:10.3233/JAD-200608

25. Zhu N, Santos-Santos M, Illán-Gala I, et al. Plasma glial fibrillary acidic protein and neurofilament light chain for the diagnostic and prognostic evaluation of frontotemporal dementia. *Transl Neurodegener*. 2021;10(1):50. doi:10.1186/s40035-021-00275-w

26. Bellaver B, Povala G, Ferreira PCL, et al. Astrocyte reactivity influences amyloid-β effects on tau pathology in preclinical Alzheimer's disease. *Nat Med*. Published online May 29, 2023. doi:10.1038/s41591-023-02380-x

27. Cicognola C, Janelidze S, Hertze J, et al. Plasma glial fibrillary acidic protein detects Alzheimer pathology and predicts future conversion to Alzheimer dementia in patients with

mild cognitive impairment. *Alzheimers Res Ther*. 2021;13(1):68. doi:10.1186/s13195-021-00804-9

28. Verberk IMW, Thijssen E, Koelewijn J, et al. Combination of plasma amyloid beta(1-42/1-40) and glial fibrillary acidic protein strongly associates with cerebral amyloid pathology. *Alzheimers Res Ther*. 2020;12(1):118. doi:10.1186/s13195-020-00682-7

29. Shir D, Graff-Radford J, Hofrenning EI, et al. Association of plasma glial fibrillary acidic protein (GFAP) with neuroimaging of Alzheimer's disease and vascular pathology. *Alzheimer's & Dementia: Diagnosis, Assessment & Disease Monitoring*. 2022;14(1). doi:10.1002/dad2.12291

30. Albert MS, DeKosky ST, Dickson D, et al. The diagnosis of mild cognitive impairment due to Alzheimer's disease: Recommendations from the National Institute on Aging-Alzheimer's Association workgroups on diagnostic guidelines for Alzheimer's disease. *Alzheimer's & Dementia*. 2011;7(3):270-279. doi:10.1016/j.jalz.2011.03.008

31. Jefferies E, Thompson H, Cornelissen P, Smallwood J. The neurocognitive basis of knowledge about object identity and events: dissociations reflect opposing effects of semantic coherence and control. *Philosophical Transactions of the Royal Society B: Biological Sciences*. 2020;375(1791):20190300. doi:10.1098/rstb.2019.0300

32. Peretti DE, Ribaldi F, Scheffler M, Chicherio C, Frisoni GB, Garibotto V. Prognostic value of imaging-based ATN profiles in a memory clinic cohort. *Eur J Nucl Med Mol Imaging*. Published online June 26, 2023. doi:10.1007/s00259-023-06311-3

33. Jovicich J, Marizzoni M, Sala-Llonch R, et al. Brain morphometry reproducibility in multi-center 3T MRI studies: A comparison of cross-sectional and longitudinal segmentations. *Neuroimage*. 2013;83:472-484. doi:10.1016/j.neuroimage.2013.05.007

34. Ashburner J, Friston KJ. Unified segmentation. *Neuroimage*. 2005;26(3):839-851. doi:10.1016/j.neuroimage.2005.02.018

35. Rolls ET, Huang CC, Lin CP, Feng J, Joliot M. Automated anatomical labelling atlas 3. *Neuroimage*. 2020;206:116189. doi:10.1016/j.neuroimage.2019.116189

36. Klunk WE, Koeppe RA, Price JC, et al. The Centiloid Project: Standardizing quantitative amyloid plaque estimation by PET. *Alzheimer's & Dementia*. 2015;11(1):1. doi:10.1016/j.jalz.2014.07.003

37. Navitsky M, Joshi AD, Kennedy I, et al. Standardization of amyloid quantitation with florbetapir standardized uptake value ratios to the Centiloid scale. *Alzheimer's & Dementia*. 2018;14(12):1565-1571. doi:10.1016/j.jalz.2018.06.1353

38. Battle MR, Pillay LC, Lowe VJ, et al. Centiloid scaling for quantification of brain amyloid with [18F]flutemetamol using multiple processing methods. *EJNMMI Res*. 2018;8(1):107. doi:10.1186/s13550-018-0456-7

39. Salvadó G, Molinuevo JL, Brugulat-Serrat A, et al. Centiloid cut-off values for optimal agreement between PET and CSF core AD biomarkers. *Alzheimers Res Ther*. 2019;11(1):1-12. doi:10.1186/s13195-019-0478-z

40. Peretti DE, Ribaldi F, Scheffler M, et al. ATN profile classification across two independent prospective cohorts. *Front Med (Lausanne)*. 2023;10. doi:10.3389/fmed.2023.1168470

41. Joachim CL, Morris JH, Selkoe DJ. Diffuse senile plaques occur commonly in the cerebellum in Alzheimer's disease. *Am J Pathol*. 1989;135(2):309-319. http://www.ncbi.nlm.nih.gov/pubmed/2675616

42. Schwarz AJ, Shcherbinin S, Slieker LJ, et al. Topographic staging of tau positron emission tomography images. *Alzheimer's and Dementia: Diagnosis, Assessment and Disease Monitoring*. 2018;10:221-231. doi:10.1016/j.dadm.2018.01.006

43. Mishra S, Gordon BA, Su Y, et al. AV-1451 PET imaging of tau pathology in preclinical Alzheimer disease: Defining a summary measure. *Neuroimage*. 2017;161:171-178. doi:10.1016/j.neuroimage.2017.07.050

44. Hoenig MC, Bischof GN, Hammes J, et al. Tau pathology and cognitive reserve in Alzheimer's disease. *Neurobiol Aging*. 2017;57:1-7. doi:10.1016/j.neurobiolaging.2017.05.004

45. Fischl B. FreeSurfer. *Neuroimage*. 2012;62(2):774-781. doi:10.1016/j.neuroimage.2012.01.021

46. Jack CR, Wiste HJ, Weigand SD, et al. Defining imaging biomarker cut points for brain aging and Alzheimer's disease. *Alzheimer's and Dementia*. 2017;13(3):205-216. doi:10.1016/j.jalz.2016.08.005

47. Palmqvist S, Janelidze S, Quiroz YT, et al. Discriminative Accuracy of Plasma Phospho-tau217 for Alzheimer Disease vs Other Neurodegenerative Disorders. *JAMA*. 2020;324(8):772. doi:10.1001/jama.2020.12134

48. Steffener J. Power of Mediation Effects Using Bootstrap Resampling. Published online June 4, 2021. http://arxiv.org/abs/2106.02482

49. Frank-Cannon TC, Alto LT, McAlpine FE, Tansey MG. Does neuroinflammation fan the flame in neurodegenerative diseases? *Mol Neurodegener*. 2009;4(1). doi:10.1186/1750-1326-4-47

50. Meraz-Ríos MA, Toral-Rios D, Franco-Bocanegra D, Villeda-Hernández J, Campos-Peña V. Inflammatory process in Alzheimer's Disease. *Front Integr Neurosci*. 2013;7(JUL). doi:10.3389/fnint.2013.00059

51. Martin JH. *Neuroanatomy Text and Atlas*. 4th ed. (Weitz M, Naglieri C, eds.). McGraw-Hill Medical; 2016.

52. Simrén J, Weninger H, Brum WS, et al. Differences between blood and cerebrospinal fluid glial fibrillary Acidic protein levels: The effect of sample stability. *Alzheimer's & Dementia*. 2022;18(10):1988-1992. doi:10.1002/alz.12806

53. Chatterjee P, Pedrini S, Ashton NJ, et al. Diagnostic and prognostic plasma biomarkers for preclinical Alzheimer's disease. *Alzheimer's and Dementia*. 2022;18(6):1141-1154. doi:10.1002/alz.12447

54. Chatterjee P, Pedrini S, Stoops E, et al. Plasma glial fibrillary acidic protein is elevated in cognitively normal older adults at risk of Alzheimer's disease. *Transl Psychiatry*. 2021;11(1). doi:10.1038/s41398-020-01137-1

55. Ashton NJ, Janelidze S, Mattsson-Carlgren N, et al. Differential roles of Aβ42/40, p-tau231 and p-tau217 for Alzheimer's trial selection and disease monitoring. *Nat Med*. 2022;28(12):2555-2562. doi:10.1038/s41591-022-02074-w

56. Bollack A, Collij LE, García DV, et al. Investigating reliable amyloid accumulation in Centiloids: Results from the AMYPAD Prognostic and Natural History Study. *Alzheimer's & Dementia*. Published online April 4, 2024. doi:10.1002/alz.13761

57. Ossenkoppele R, van der Flier WM. APOE Genotype in the Era of Disease-Modifying Treatment With Monoclonal Antibodies Against Amyloid-β . *JAMA Neurol*. Published online November 6, 2023. doi:10.1001/jamaneurol.2023.4046

58. Pemberton HG, Collij LE, Heeman F, et al. Quantification of amyloid PET for future clinical use: a state-of-the-art review. *Eur J Nucl Med Mol Imaging*. Published online 2022. doi:10.1007/s00259-022-05784-y

59. Ossenkoppele R, Smith R, Mattsson-Carlgren N, et al. Accuracy of Tau Positron Emission Tomography as a Prognostic Marker in Preclinical and Prodromal Alzheimer Disease. *JAMA Neurol*. 2021;78(8):961. doi:10.1001/jamaneurol.2021.1858

60. Villemagne VL, Leuzy A, Bohorquez SS, et al. CenTauR: Toward a universal scale and masks for standardizing tau imaging studies. *Alzheimer's & Dementia: Diagnosis, Assessment & Disease Monitoring*. 2023;15(3). doi:10.1002/dad2.12454

61. Yang H, Xu H, Li Q, et al. Study of brain morphology change in Alzheimer's disease and amnestic mild cognitive impairment compared with normal controls. *Gen Psychiatr*. 2019;32(2):e100005. doi:10.1136/gpsych-2018-100005

62. Thompson PM, Mega MS, Woods RP, et al. Cortical Change in Alzheimer's Disease Detected with a Disease-specific Population-based Brain Atlas. *Cerebral Cortex*. 2001;11(1):1-16. doi:10.1093/cercor/11.1.1

63. Lubben N, Ensink E, Coetzee GA, Labrie V. The enigma and implications of brain hemispheric asymmetry in neurodegenerative diseases. *Brain Commun*. 2021;3(3). doi:10.1093/braincomms/fcab211

64. Franzmeier N, Rubinski A, Neitzel J, et al. Functional connectivity associated with tau levels in ageing, Alzheimer's, and small vessel disease. *Brain*. 2019;142(4):1093-1107. doi:10.1093/brain/awz026

65. Smith R, Schöll M, Leuzy A, et al. Head-to-head comparison of tau positron emission tomography tracers [18F]flortaucipir and [18F]RO948. *Eur J Nucl Med Mol Imaging*. 2020;47(2):342-354. doi:10.1007/s00259-019-04496-0

66. Gogola A, Minhas DS, Villemagne VL, et al. Direct Comparison of the Tau PET Tracers ^{18}F-Flortaucipir and ^{18}F-MK-6240 in Human Subjects. *Journal of Nuclear Medicine*. 2022;63(1):108-116. doi:10.2967/jnumed.120.254961

67. Sims JR, Zimmer JA, Evans CD, et al. Donanemab in Early Symptomatic Alzheimer Disease. *JAMA*. 2023;330(6):512. doi:10.1001/jama.2023.13239

68. van Dyck CH, Swanson CJ, Aisen P, et al. Lecanemab in Early Alzheimer's Disease. *New England Journal of Medicine*. 2023;388(1):9-21. doi:10.1056/NEJMoa2212948

69. Bateman RJ, Cummings J, Schobel S, et al. Gantenerumab: an anti-amyloid monoclonal antibody with potential disease-modifying effects in early Alzheimer's disease. *Alzheimers Res Ther*. 2022;14(1):178. doi:10.1186/s13195-022-01110-8

70. Ji C, Sigurdsson EM. Current Status of Clinical Trials on Tau Immunotherapies. *Drugs*. 2021;81(10):1135-1152. doi:10.1007/s40265-021-01546-6

Figure Legends

Figure 1 Distribution of GFAP by AT status and its correlation with AT biomarkers. Distribution of plasma GFAP levels by AT status and association between GFAP and AT biomarkers: **(A)** boxplots containing the distribution of plasma GFAP levels by AT status. Boxes represent the interquartile range of values; the horizontal line, the median score per group; whiskers expand up to 1.5 times the interquartile range; remaining black dots correspond to outliers. Coloured circles represent individual values. Significant differences between groups are marked by a horizonal square bracket with respective *P*-values. **(B)** A scatter plot showing the correlation between Centiloid and plasma GFAP values. **(C)** A scatter plot showing the correlation between global tau SUVR and plasma GFAP levels. In both scatter plots (**A** and **B**), the black line represents the linear regression between variables. In all plots, dot colours are defined by AT status: A-T- in green, A-T+ in yellow, A+T- in blue, and A+T+ in red.

Figure 2 Voxel-wise association between tau and GFAP. Association between plasma GFAP and tau PET SUVR uptake independently of Centiloid. Statistical parametric maps were investigated at $P < 0.001$ with FWE-corrected at cluster level. Age, gender, years of education, and APOE carriership were used as covariates in the model.

Figure 3 Mediation analysis results. Path diagrams indicate whether plasma GFAP mediated the association between **(A)** Centiloid and global tau SUVR, and **(B)** global tau SUVR and the annual rate of MMSE change, adjusted for age, gender, education, cortical thickness, and **(A)** MMSE scores, or **(B)** Centiloid. The direct effect reflects the extent to which **(A)** global tau SUVR or **(B)** annual rate of MMSE change changes when baseline **(A)** Centiloid or **(B)** global tau SUVR increases by 1 unit while baseline plasma GFAP remains unaltered. The indirect effect reflects the extent to which **(A)** global tau SUVR or **(B)** annual

rate of MMSE change changes when baseline **(A)** Centiloid or **(B)** global tau SUVR is held constant and plasma GFAP levels change by the amount it would have changed had baseline **(A)** Centiloid or **(B)** global tau SUVR increased by 1 unit. The total effect is the sum of direct and indirect effects. Asterisks mark statistically significant values.

Table 1 Demographic, cognitive, imaging characteristics, and plasma GFAP levels at baseline of subjects included in the study

AT Status	A−T− (n = 47)	A−T+ (n = 3)	A+T− (n = 28)	A+T+ (n = 44)	*P*−value
Age (years)	70 ± 8	76 ± 5	74 ± 8	74 ± 7	0.04
Gender (F/M)	23/24	3/0	8/20	27/17	0.01
Education (years)	15 ± 4	11 ± 1	15 ± 4	13 ± 4	0.14
MMSE at Baseline	27 ± 2[a]	28 ± 2	27 ± 2[a]	24 ± 5[b]	<0.01
Diagnosis Stage (CU/MCI/Dementia/Other)	21/19/2/5	2/1/0/0	5/19/4/0	1/31/12/0	<0.01
APOE Carriership (Non-Carrier/Carrier)	40/7	3/0	20/8	12/32	<0.01
Centiloid	−2 ± 8[b,d]	−3 ± 11[b,d]	50 ± 29[b,c]	81 ± 32[a]	<0.01
Global Tau SUVR	1.14 ± 0.09[b]	1.35 ± 0.03	1.18 ± 0.11[b]	1.67 ± 0.36[a]	<0.01
Composite AD Cortical Thickness Signature (mm)	2.78 ± 0.13[a]	2.78 ± 0.18	2.70 ± 0.18	2.62 ± 0.20[b]	<0.01
Plasma GFAP (pg/ml)	128 ± 97[b]	170 ± 12	201 ± 115[a]	246 ± 104[a]	<0.01

Reported *P*-values result from Kruskal-Wallis. Dunn tests for post-hoc analysis using Benjamin-Hochberg correction for multiple comparisons were used to compare between groups. Superscript letters indicate groups showing significant differences at post-hoc comparison: a > b, c > d. A = Amyloid, T = Tau, n = number of subjects, F = female, M = male, MMSE = Mini-Mental State Examination, CU = Cognitively Unimpaired, MCI = Mild Cognitive Impairment, SUVR = Standardised Uptake Value Ratio, AD = Alzheimer's Disease, mm = millimetres, GFAP = Glial Fibrillary Acidic Protein.

Table 2 Correlation coefficients of Alzheimer's disease biomarkers or MMSE score with plasma GFAP levels

Biomarker	Correlation Coefficient	*P*-value
Centiloid	0.46	<0.01
Global VOI Tau SUVR	0.48	<0.01
Braak I/II VOI Tau SUVR	0.22	0.02
Braak III VOI Tau SUVR	0.46	<0.01
Braak IV VOI Tau SUVR	0.44	<0.01
Braak V VOI Tau SUVR	0.35	<0.01
Braak VI VOI Tau SUVR	0.17	0.06
Composite AD Cortical Thickness Signature	-0.34	<0.01
Baseline MMSE score	-0.34	<0.01

Spearman correlation coefficients of Alzheimer's disease imaging biomarkers or MMSE score with plasma GFAP levels at baseline. VOI = Volume of Interest, SUVR = Standardised Uptake Value Ratio, AD = Alzheimer's Disease, MMSE = Mini-Mental State Examination.

Table 3 Correlation coefficients of Alzheimer's disease biomarkers or GFAP levels with MMSE annual rate of change

Biomarker	Correlation Coefficient	*P*-value
Centiloid	0.41	<0.01
Global VOI Tau SUVR	0.43	<0.01
Braak I/II VOI	0.27	<0.01
Braak III VOI	0.47	<0.01
Braak IV VOI	0.44	<0.01
Braak V VOI	0.33	<0.01
Braak VI VOI	0.13	0.20
Composite AD Cortical Thickness Signature	-0.38	<0.01
Plasma GFAP	0.46	<0.01

Spearman correlation coefficients of Alzheimer's disease imaging biomarkers or plasma GFAP levels with MMSE annual rate of change.
VOI = Volume of Interest, SUVR = Standardised Uptake Value Ratio, AD = Alzheimer's Disease, MMSE = Mini-Mental State Examination

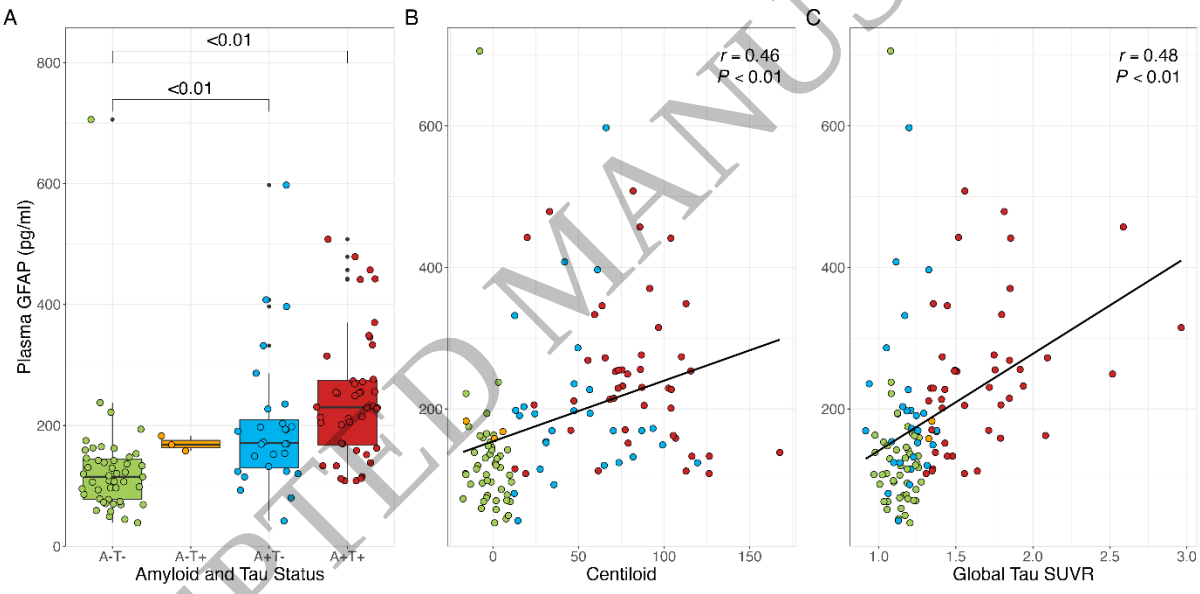

Figure 1
470x229 mm (x DPI)

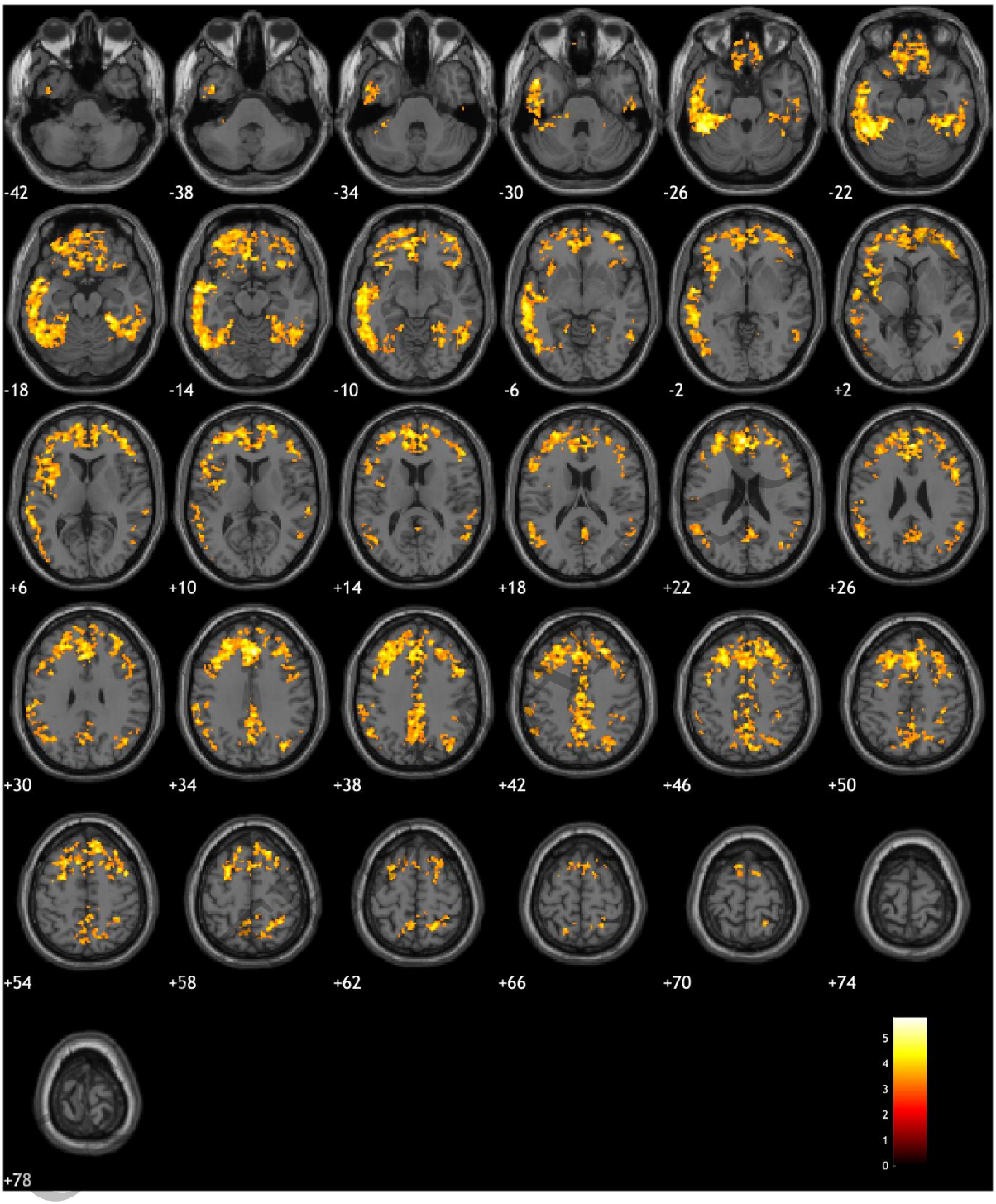

Figure 2
228x273 mm (x DPI)

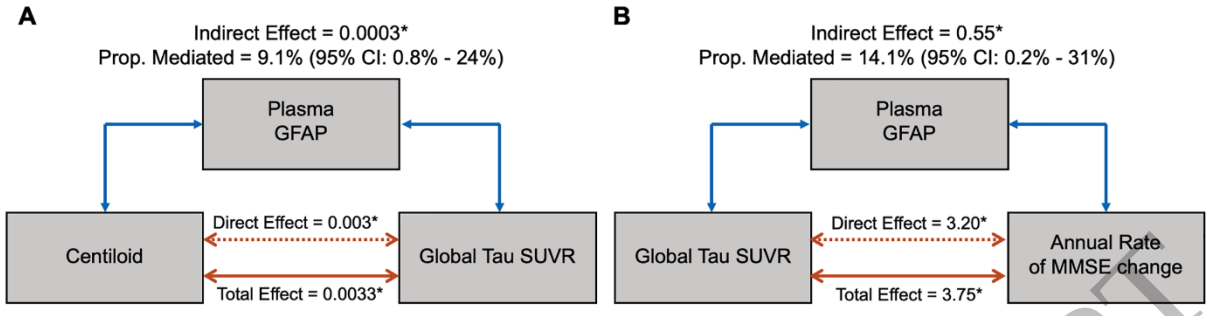

Figure 3
200x56 mm (x DPI)